# Temperature Dependence of Raman Linewidth and Shift in α-Quartz*

A. S. Pine and P. E. Tannenwald
*Lincoln Laboratory, Massachusetts Institute of Technology, Lexington, Massachusetts 02173*

(Received 30 September 1968)

The linewidth and frequency of the 128-cm$^{-1}$ and the 466-cm$^{-1}$ optical lattice vibrations in quartz have been measured between 5 and 300°K by means of high-resolution Raman spectroscopy. The 128-cm$^{-1}$ mode, which is both Raman- and infrared-active, is the lowest-lying optical vibration in quartz and shows a marked increase in lifetime at low temperatures. Utilizing available phonon dispersion spectra obtained from neutron scattering, the linewidth and shift are calculated in terms of three-phonon interactions. A simple model for the cubic anharmonicity, which includes relaxation broadening of the thermal phonons, is applied satisfactorily to the residual damping at low temperatures. The 128-cm$^{-1}$ LO-TO splitting, which is extremely small, is not resolved directly, but manifests itself as an observed broadening at helium temperatures.

## 1. INTRODUCTION

HIGH-RESOLUTION Raman scattering has been used to measure the linewidth and frequency of two optical lattice vibrations in crystalline quartz from 5 to 300°K. The vibrations studied were the infrared-active, 128-cm$^{-1}$ species-$E$ mode and the infrared-inactive 466-cm$^{-1}$ species-$A_1$ mode. The temperature variation can be explained in terms of simple anharmonic effects involving only three-phonon processes.

The 128-cm$^{-1}$ mode is particularly interesting since it is the lowest-lying optical vibration in quartz. At very low temperatures its lifetime increases markedly as it can decay only into a relatively low density of acoustic phonon states. A model calculation, generalized to include the possibility of broadened acoustic modes, gives a rough numerical estimate of this residual width. At higher temperatures, scattering of thermal acoustic and optical phonons dominates the damping of the 128-cm$^{-1}$ vibration. Assignment of the most likely channels for decay and scattering of the 128- and 466-cm$^{-1}$ modes is made possible by recent neutron scattering data of phonon dispersion in quartz.

Of corollary interest is a determination of the polariton properties of the 128-cm$^{-1}$ vibration. Generally, the degeneracy of the longitudinal and transverse components of $E$-symmetry modes is lifted by the coupling of the effective charge to the electromagnetic field. The resultant splitting, if measurable, determines this coupling and, thereby, the phonon-photon admixture and the dispersion of the excitation. However, the 128-cm$^{-1}$ mode is only weakly infrared active. The room-temperature oscillator strength, measured by far infrared spectroscopy, yields a splitting much smaller than the natural linewidth. As the temperature is lowered, it is known qualitatively that the infrared absorption decreases, but at a slower rate than the linewidth. Unfortunately, even at liquid-helium temperatures, the splitting is never fully resolved from the natural linewidth. An approximate value of the low-temperature oscillator strength may be obtained, though, because a broadening of the pure-mode width is evident when both longitudinal and transverse components contribute to the Raman scattering.

Although the Raman and infrared spectra of quartz have been studied for years, the proper interpretation of the modes has only recently been established by Kleinman and Spitzer,[1] Elcombe,[2] and Scott and Porto.[3] The latter paper contains an extensive bibliography of the previous work. The polariton effects have since been illuminated by Scott, Cheesman, and Porto.[4] Recently a controversial feature of the spectrum has been classified by Scott[5] as an enhanced second-order scattering by anharmonically coupled one and two phonon states. Earlier, Shapiro, O'Shea, and Cummins[6] had observed that the extra mode was implicated in the $\alpha$-$\beta$ phase transition of quartz and suggested an asymmetric double-well or twinning model to explain these observations. The nature of the $\alpha$-$\beta$ transition was the inspiration for several early experiments on the temperature dependence of the Raman shift and linewidth. Of these, Nedungadi[7] and Narayanaswamy[8] cataloged the thermal variations in quartz most completely. The simple anharmonic properties were in evidence then but were not analyzed. This present work may be regarded as an extension of the Indian work with the advantages of lasers and higher resolution apparatus, a theoretical model of anharmonic effects, and lower temperatures to help sort out these effects. Zubov and Osipova[9] achieved the resolution necessary for a careful study of the 300°K quartz Raman spectrum. An improvement of two orders of magnitude, required for the 5°K, 128-cm$^{-1}$ mode, is accomplished here by low dark-count photoelectric detection of the spectrum analyzed by a pressure-scanned Fabry-Perot interferometer. The 466-cm$^{-1}$ mode, on the other hand, is

* Work sponsored by the U. S. Air Force.

[1] D. A. Kleinman and W. G. Spitzer, Phys. Rev. **125**, 16 (1962).
[2] M. M. Elcombe, Proc. Phys. Soc. (London) **91**, 947 (1967).
[3] J. F. Scott and S. P. S. Porto, Phys. Rev. **161**, 903 (1967).
[4] J. F. Scott, L. E. Cheesman, and S. P. S. Porto, Phys. Rev. **162**, 834 (1967).
[5] J. F. Scott, Phys. Rev. Letters **21**, 907 (1968).
[6] S. M. Shapiro, D. C. O'Shea, and H. Z. Cummins, Phys. Rev. Letters **19**, 361 (1967).
[7] T. M. K. Nedungadi, Proc. Indian Acad. Sci. **A11**, 86 (1940).
[8] P. K. Narayanaswamy, Proc. Indian Acad. Sci. **A26**, 521 (1947).
[9] V. G. Zubov and L. P. Osipova, Kristallografiya **6**, 418 (1961) [English transl.: Soviet Phys.—Crist. **6**, 330 (1961)].

always broad enough to be resolved with available grating spectrometers, but its thermal shift at cryogenic temperatures is unmeasurably small for the precision of the grating scanner mechanism. Here, the technique of stimulated Raman scattering is used to artificially sharpen and intensify the line for interferogram readout.

The temperature dependence of Raman linewidths has been measured in other crystals using laser spectroscopy. Park[10] has examined calcite, and Ralston, Keating, and Chang[11] have studied silicon and gallium arsenide. As for the case of the 466-cm$^{-1}$ mode in quartz, the resolution of a grating spectrometer was sufficient at all temperatures for these solids.

## 2. THEORETICAL DISCUSSION

### A. Anharmonic Effects

The Raman spectrum of light scattered from an anharmonic crystal depends on the Fourier transform of the space-time phonon amplitude correlation function. This correlation function is subject to the dynamics of the anharmonic interaction which imparts a complex energy shift to the lattice vibration. If $\mathbf{q}$ and $j$ are the wave vector and branch of the phonon observed, then the normalized spectral distribution is $(\Gamma_{qj}/\pi)/[(\omega_s-\omega_I\pm\omega_{qj}\pm\Delta_{qj})^2+\Gamma_{qj}^2]$. Here, $\omega_I$ and $\omega_s$ are the incident and scattered light frequencies, and $\omega_{qj}$ is the frequency of the phonon mode in a perfectly harmonic lattice. The anharmonicity causes a shift $\Delta_{qj}$ in the peak of the line and a finite width $\Gamma_{qj}$ corresponding to the damping of the vibration. Both quantities are temperature-dependent through the thermal population factors of the interacting phonons.

General expressions for the shift and damping have been derived by several authors using the thermal Green's-function techniques of many-body theory.[12–14] Previous derivations, using first-order perturbation theory for $\Gamma$ and second order for $\Delta$, gave similar results,[15–17] but the boson factors were treated artificially and no consideration was given to the relaxation broadening or "dressing" of the thermal phonons.

The results of the Green's-function theory for the shift and damping are

$$\Delta_{qj}=\frac{\hbar}{16m^3\omega_{qj}}\frac{\Omega}{(2\pi)^3}P\int d^3q_1\sum_{j_1j_2}\frac{|\Phi_{jj_1j_2}(\mathbf{q}\mathbf{q}_1\mathbf{q}_2)|^2}{\omega_{q_1j_1}\omega_{q_2j_2}}\times\Delta(\mathbf{q}+\mathbf{q}_1+\mathbf{q}_2)\{-(n_1+n_2+1)/(\omega_{qj}+\omega_{q_1j_1}+\omega_{q_2j_2})+(n_1+n_2+1)/(\omega_{qj}-\omega_{q_1j_1}-\omega_{q_2j_2})-(n_1-n_2)/(\omega_{qj}-\omega_{q_1j_1}+\omega_{q_2j_2})+(n_1-n_2)/(\omega_{qj}+\omega_{q_1j_1}-\omega_{q_2j_2})\}, \quad (1)$$

$$\Gamma_{qj}=\frac{\pi\hbar}{16m^3\omega_{qj}}\frac{\Omega}{(2\pi)^3}\int d^3q_1\sum_{j_1j_2}\frac{|\Phi_{jj_1j_2}(\mathbf{q}\mathbf{q}_1\mathbf{q}_2)|^2}{\omega_{q_1j_1}\omega_{q_2j_2}}\times\Delta(\mathbf{q}+\mathbf{q}_1+\mathbf{q}_2)\{-(n_1+n_2+1)\delta(\omega_{qj}+\omega_{q_1j_1}+\omega_{q_2j_2})+(n_1+n_2+1)\delta(\omega_{qj}-\omega_{q_1j_1}-\omega_{q_2j_2})-(n_1-n_2)\delta(\omega_{qj}-\omega_{q_1j_1}+\omega_{q_2j_2})+(n_1-n_2)\delta(\omega_{qj}+\omega_{q_1j_1}-\omega_{q_2j_2})\}. \quad (2)$$

$P$ represents the principal part; $\Delta(\mathbf{q}+\mathbf{q}_1+\mathbf{q}_2)$ states that wave vector must be conserved up to a reciprocal lattice vector; $m$ and $\Omega$ are the mass and volume of the crystal; $n_i=[\exp(\hbar\omega_{q_ij_i}/kT)-1]^{-1}$ is the thermal population factor. The frequencies of the purely harmonic lattice are not actually observable once the interaction is present. If the shifts are much less than the harmonic frequencies, then it is a good approximation to replace $\omega_{q_ij_i}$ with $\omega_i$, the low-temperature frequencies, where unnecessary indices have been suppressed.

$\Phi$ is the Fourier transform of the cubic coefficient in the expansion of the lattice potential energy. With slight change of notation, $\Phi$ is defined by Kwok,[14] and Born and Huang.[18] We have dropped quartic and higher terms and consider only three phonon processes. We take for our model

$$\Phi_{jj_1j_2}(\mathbf{q}\mathbf{q}_1\mathbf{q}_2)=\gamma_{jj_1j_2}(m/c)\omega_{qj}\omega_{q_1j_1}\omega_{q_2j_2}A_{jj_1j_2}^{\hat{q}\hat{q}_1}, \quad (3)$$

where $c$ is a typical acoustic velocity, $A$ is an anisotropy factor depending only on the direction of the wave vectors, and $\gamma$ is a dimensionless constant measuring the anharmonicity. This expression, though introduced as an ansatz, leads to the standard definition for $\gamma$ as the Grüneisen constant in the acoustic continuum limit.

The derivation of the shift and linewidth above is the lowest order approximation in the anharmonicity since self-energy contributions to the "bare" phonons at $\omega_{q_ij_i}$ have been neglected. This approximation is often inadequate, and it becomes necessary to "dress" these modes with their own collisions by resorting to higher-order perturbation theory or diagrams. The result of such a calculation is to endow these phonons with a finite lifetime or damping. It is shown by Kwok[14] that this circumstance may be treated by simply substituting, in Eq. (2), the convolved spectral representation of the $\delta$ function

$$\delta(\omega\pm\omega_1\pm\omega_2)\rightarrow[(\Gamma_1+\Gamma_2)/\pi]/[(\omega\pm\omega_1\pm\omega_2)^2+(\Gamma_1+\Gamma_2)^2], \quad (4)$$

[10] K. Park, Phys. Letters **25A**, 490 (1967).
[11] J. M. Ralston, D. E. Keating, and R. K. Chang, in *Light Scattering in Solids*, edited by G. B. Wright (to be published).
[12] A. A. Maradudin and A. E. Fein, Phys. Rev. **128**, 2589 (1962).
[13] R. A. Cowley, *Phonons in Perfect Lattices and in Lattices with Point Imperfections*, edited by R. W. H. Stevenson (Plenum Press, Inc., New York, 1966).
[14] P. C. Kwok, Ph.D. thesis, Harvard University, 1965 (unpublished).
[15] D. A. Kleinman, Phys. Rev. **118**, 118 (1960).
[16] R. Loudon, Proc. Roy. Soc. (London) **A275**, 218 (1963).
[17] P. G. Klemens, Phys. Rev. **148**, 845 (1966).
[18] M. Born and K. Huang, *Dynamical Theory of Crystal Lattices* (Oxford University Press, London, 1962).

where $\Gamma_i$ is the damping rate of mode $\omega_i$. Such broadening of the interaction phonons may have interesting physical consequences, as will be shown in an example. For quartz, the effect on the Raman linewidths is small, but the effect on the acoustic modes is crucial.[14,19]

Interpretation of Eqs. (1) and (2) in terms of three-phonon interactions is relatively straightforward. The first term in the curly brackets is a simultaneous absorption of all three phonons. This cannot conserve energy and is nowhere near resonance, so the process may be ignored. The second term is the decay of the observed phonon into two lower energy phonons and accounts for the residual shift and width at low temperatures. The third and fourth terms are equivalent by exchange of the dummy indices $1 \leftrightarrow 2$ and represent a scattering of a thermal phonon by the observed phonon. In all cases the emission processes are automatically subtracted from the absorption processes in the many-body derivation.

The difficulty in evaluating (1) and (2) for a real material is that the parameters $\gamma$, $A$, and $\Gamma_i$ are generally unknown, and even the modes $\omega_i$ may not be established throughout the Brillouin zone. Fortunately, the resonance character of the integrals and/or the flatness of the optical phonon bands allow the temperature factors to be removed from the integral. Comparison with experiment can then be made, and the remaining unknown integrals adjusted to fit the data. All that is required for this procedure is a rough knowledge of the phonon dispersion, which is now available for quartz.

At very low temperatures all the $n_i \to 0$, so only the decay terms contribute to the anharmonicity. The number of processes for the damping is strictly limited because of the energy-conservation requirement. On the other hand, the shift is not so restricted and the problem becomes difficult to analyze. In fact, since the zero-temperature shift, unlike the residual damping, is unmeasurable, there is little reason for a detailed calculation. Therefore the model Eq. (3) is best tested on the damping.

The situation is more complex as the temperature is raised since more modes, which are candidates for interaction, become thermally populated. At very high temperatures all processes go simply as $n_i \to kT/\hbar\omega_i$, and there is virtually no hope of unraveling the contributions of the individual channels.

We now consider the decay of an optical phonon at $\mathbf{q}=0$ into two acoustic phonons of equal energy and opposite wave vector. This example is pertinent to the low-temperature damping of the 128-cm$^{-1}$ Raman mode in quartz. To simplify the calculation, elastic isotropy is assumed. Thus $\omega_i$ is a function only of the magnitude of $\mathbf{q}_i$; and $A$ is set equal to one. This assumption should not lead to large errors unless critical points in the acoustic branches are involved in the decay, and they are distributed very anisotropically in the real crystal. With these provisions, we insert (3) and (4) into the decay term of (2):

$$\Gamma_0=\frac{\hbar\gamma^2}{16\rho}\frac{\omega_0}{c^2}\frac{2}{(2\pi)^3}\int d^3q_1\omega_1^2(2n_1+1)\Gamma_1/[(\omega_0-2\omega_1)^2+(2\Gamma_1)^2]. \quad (5)$$

Here, the density $\rho=m/\Omega$. We expand $\omega_1=\frac{1}{2}(\omega_0)+(\partial\omega_1/\partial q_1)_{\omega_0/2}(q_1-q_0)$, where $q_0$ is the wave vector on the $\omega_1$ branch corresponding to $\frac{1}{2}\omega_0$. The slowly varying boson factor $n_1$ and the damping $\Gamma_1$ may be evaluated at $\frac{1}{2}\omega_0$. We define the group velocity $c_g=(\partial\omega_1/\partial q_1)_{\omega_0/2}$ and the attenuation $\alpha=(\Gamma_1/c_g)_{\omega_0/2}$. The angular integrations are trivial in this isotropic case, and if we ignore the unimportant dispersion in the numerator (setting $\omega\sim cq_1$), then we have

$$\Gamma_0=\frac{\hbar\gamma^2}{16\rho}\frac{\omega_0\alpha}{c_g}\frac{(2n_1+1)_{\omega_0/2}}{(2\pi)^2}\int_0^Q q_1^4dq_1/[(q_1-q_0)^2+\alpha^2]. \quad (6)$$

Here $Q$ is the Brillouin zone edge wave vector. The remaining integration is an elementary form and the answer may be expressed conveniently if we define the following parameters:

$$\Gamma_0^0=(\hbar\gamma^2/64\pi\rho)(\omega_0/c_g)q_0^4, \quad (7a)$$

$$n_0=(n_1)_{\omega_0/2}, \quad \eta=\alpha/q_0, \quad \delta=Q/q_0. \quad (7b)$$

Then (6) becomes

$$\Gamma_0=(2n_0+1)\Gamma_0^0F(\eta,\delta), \quad (8)$$

where

$$F(\eta,\delta)=\left\{(1-6\eta^2+\eta^4)\left[\tan^{-1}\left(\frac{\delta-1}{\eta}\right)+\tan^{-1}\left(\frac{1}{\eta}\right)\right]+(\tfrac{1}{3}\eta\delta^3+\eta\delta^2+3\eta\delta-\eta^3\delta)+(2\eta-2\eta^3)\ln\left|\frac{(\delta-1)^2+\eta^2}{1+\eta^2}\right|\right\}. \quad (9)$$

Now $\Gamma_0^0$ would be the residual low-temperature damping in the absence of the broadening $\Gamma_1$. This factor diverges if the decay occurs at a critical point where $c_g=0$. In fact, such behavior signals the breakdown of first-order perturbation theory. However, when $\Gamma_1$ is finite a simultaneous divergence of $\alpha$ and $\eta$ prevents $\Gamma_0$ from blowing up. For this critical point decay, we then have

$$\Gamma_0=(\hbar\gamma^2/320\pi^2\rho)(\omega_0/\Gamma_1)Q^5(2n_0+1) \quad (10)$$

and the damping is *reduced* as a consequence of the acoustic broadening. Far from the critical point where $c_g\sim c$, we have $\eta\sim 2\Gamma_1/\omega_0 \ll 1$, and $F$ can be greater or less than one. For example, if also $\eta \ll \delta-1$, then to

[19] A. S. Pine, in *Light Scattering in Solids*, edited by G. B. Wright (to be published).

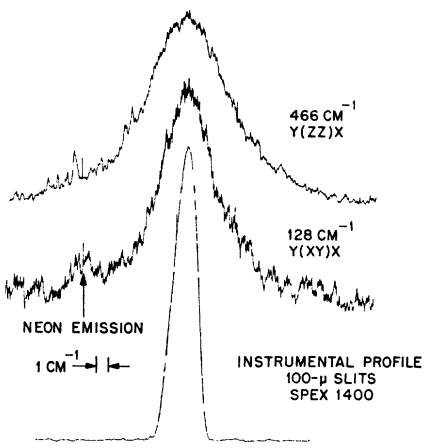


FIG. 1. 300°K Raman vibrations in α-quartz. Grating spectrometer.

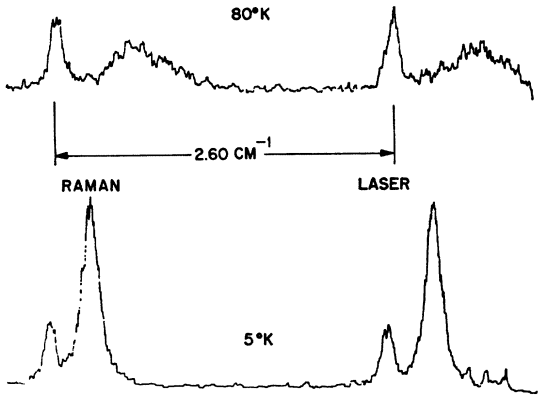


FIG. 2. 128-cm$^{-1}$ LO Raman line in α-quartz backscattered along $x$ axis. Fabry-Perot interferometer.

first order in $\eta$,

$$F(\eta,\delta)=\left\{1+\frac{\eta}{\pi}\left[\tfrac{1}{3}\delta^3+\delta^2+3\delta-(\delta/(\delta-1))+4\ln(\delta-1)\right]\right\}. \quad (11)$$

For the decay of the 128-cm$^{-1}$ mode in quartz $\delta\sim 2$ or 3, and the damping is *increased* as a result of acoustic broadening. To summarize, the effect of $\Gamma_1$ is to reduce the coupling in those channels which exactly conserve energy, but to make possible communication with new states which are slightly off resonance. If there is a low density of conserving states, then there is usually an enhancement of the decay process.

Calculation of the decay processes to lower optical branches, if available, and of the scattering processes may proceed in the same way. Of course, the handicap of unknown parameters is usually worse the higher up in the phonon spectrum one goes. It should be mentioned that the decay model derived in (8) is the only possible damping mechanism for simpler crystals such as diamond or silicon.

### B. Polaritons

The polariton problem in quartz has been thoroughly discussed by Kleinman and Spitzer[1] and Scott, Cheesman, and Porto.[4] We recount some of the formulas here that will be useful for discussing the 128-cm$^{-1}$ vibration.

Classical dispersion of the mixed infrared and $E$-symmetry vibrations can be expressed by a complex dielectric constant for the ordinary polarization

$$\epsilon(\omega)=\epsilon_\infty+\sum_i s_i\omega_i^2/(\omega_i^2-\omega^2-i\Gamma_i\omega), \quad (12)$$

where $\epsilon_\infty$ is the optical dielectric constant and $i$ runs over the eight species $E$ modes. $s_i$ is the oscillator strength of the mode at $\omega_i$ and can be written in terms of an effective ionic charge $e_i^*$, a reduced mass $\mu_i$, and the unit cell volume $\Omega_0$:

$$s_i=e_i^*/4\pi^2\mu_i\omega_i^2\Omega_0. \quad (13)$$

In the absence of damping, $\epsilon$ is real; the transverse frequencies are given by the poles of $\epsilon$ at $\omega_{ti}=\omega_i$ and the longitudinal components $\omega_{li}$ are given by the zeros. This results in a splitting $\bar{\omega}_i=\omega_{li}-\omega_{ti}$ which, if it is small compared to $\omega_i$, we have

$$\bar{\omega}_i\simeq\tfrac{1}{2}s_i\omega_i\Big/\left[\epsilon_\infty+\sum_{j\neq i}\frac{s_j\omega_j^2}{\omega_j^2-\omega_i^2}\right]. \quad (14)$$

The bracketed denominator is the contribution from all other modes to the dielectric constant at frequency $\omega_i$. For the 128-cm$^{-1}$ mode in quartz this is nearly $\epsilon_0$, the static value.

Like the vibrational frequency and linewidth, the oscillator strength is also temperature-dependent. This is another effect of anharmonicity since a pure-mode wave function can be modified by coupling to pairs of other modes of more or less effective charge.[20] We note also that the LO and TO components may differentially shift according to Eq. (1) since there may be differing selection rules and differing energy denominators in cases where the two modes are highly split. Thus the splitting, hence the oscillator strength, may vary with temperature.

## 3. EXPERIMENTAL RESULTS AND ANALYSIS

Three experimental systems were used to obtain the results reported here. The first was a conventional Raman spectrometer employing a 20-mW He-Ne laser, a tandem Spex grating monochromator, and a cooled EMI 9558B photomultiplier (PM). The discriminated output of the PM was integrated and displayed on a strip chart. With 100-μ slits, the linewidths of the

[20] H. Bilz, in *Phonons in Perfect Lattices and in Lattices with Point Imperfections*, edited by R. W. H. Stevenson (Plenum Press, Inc., New York, 1966).

128-cm$^{-1}$ mode above 200°K and the 466-cm$^{-1}$ mode for all temperatures were resolved. Room-temperature traces are shown in Fig. 1. Linewidths were obtained by convolving Lorentzian lines with the instrumental profile and fitting to the experimentally observed spectra. The large frequency shifts above liquid-nitrogen temperature could be measured with this system. However, absolute frequencies could not be calibrated to better than $\pm 1$ cm$^{-1}$ because of nonlinearities and inconsistencies in the grating drive. For this same reason, the shifts at low temperatures had to be measured by interferometry with normalization to the frequencies at 80°K.

To accomplish this measurement, a second experiment was performed utilizing stimulated Raman scattering from quartz powered by a 10-MW ruby laser. This apparatus and properties of the Raman output have been described elsewhere.[21] The 466-cm$^{-1}$ mode could be stimulated over a temperature range from 5 to 240°K, and the Raman shift could be measured precisely on a Fabry-Perot interferogram. Stimulation of the 128-cm$^{-1}$ mode could also be achieved at low temperatures.

The low-temperature linewidth, shift, and oscillator strength of the 128-cm$^{-1}$ mode were measured in a third, high-resolution, apparatus. Here the backscattered Raman spectrum was analyzed by a pressure-scanned Fabry-Perot interferometer. The excitation source was the 20-mW He-Ne laser; isolation of the Raman line of interest was accomplished by interference filters; and

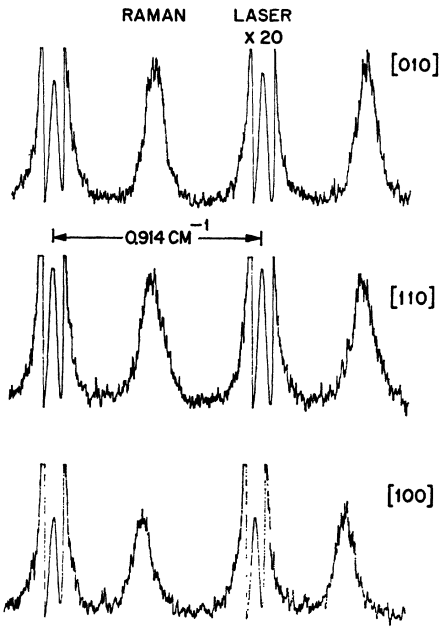


FIG. 3. 128-cm$^{-1}$ Raman line in $\alpha$-quartz backscattered along three principal axes at 5°K. High-resolution Fabry-Perot interferometer.

[21] P. E. Tannenwald, J. Appl. Phys. 38 4788 (1967).

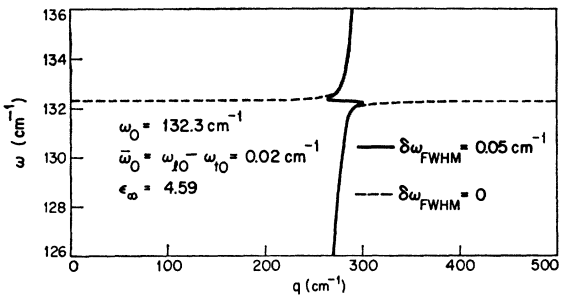


FIG. 4. Zone-center polariton-dispersion relation for 128-cm$^{-1}$ $E$ mode in $\alpha$-quartz at 5°K with and without damping. In the presence of damping the full lossless dispersion may be observed by Raman scattering.

the scanned spectrum was detected by a low-noise, uncooled ITT FW130 photomultiplier with discriminated output. A similar spectrometer was developed by Clements and Stoicheff[22] to measure narrow Raman vibrations in liquids. Backscattering was selected over 90° scattering because of greater light collection efficiency when matched to a Fabry-Perot. Of course, the extraneous surface scattered laser light was more severe in this geometry.

Typical traces are shown in Figs. 2 and 3. In Fig. 2 we see the effect of temperature on the Raman shift

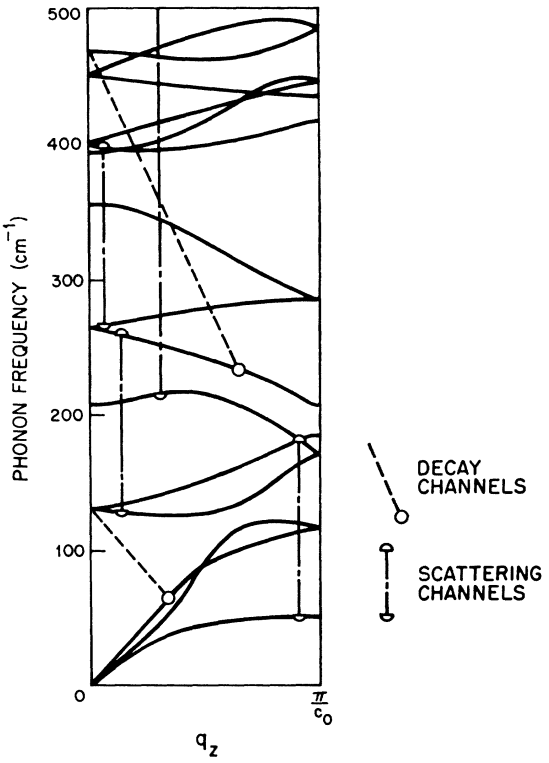


FIG. 5. Dispersion relations for selected phonons along trigonal axis in $\alpha$-quartz. Based on data of Elcombe (Ref. 2).

[22] W. R. L. Clements and B. P. Stoicheff, Appl. Phys. Letters 12, 246 (1968).

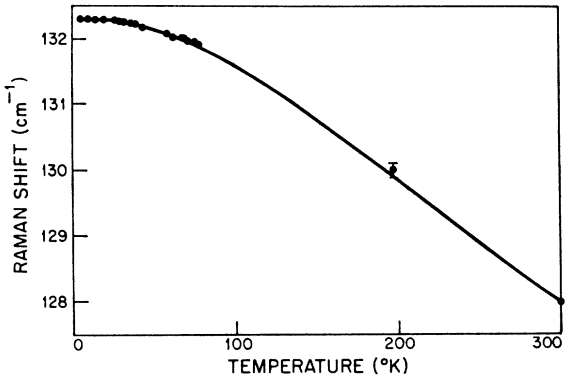


FIG. 6. Raman shift of 128-cm$^{-1}$ mode in $\alpha$-quartz. The solid curve is $\Delta_{132}=(2n_{66}+1)0.42+(n_{266}-n_{398})10$.

and width. The laser light leakage acts as a marker for the free spectral range of 2.60 cm$^{-1}$. Only the Stokes line appears because of the filtering and the low temperature.

Figure 3 displays higher-resolution, helium-temperature spectra for various crystal phonon propagation directions. In each case the incident and the scattered light are polarized in the ordinary ray. Anisotropic and electrostatic properties of the scattering are illustrated by these traces. Examination of the Raman tensor and phonon polarization given by Loudon[23] demonstrates that the scattered intensity from the longitudinal branch goes as $I_l\cos^2 3\psi$ and the transverse branch as $I_t\sin^2 3\psi$, where $\psi$ is measured between the [100] axis and the phonon wave vector. In general, $I_l$ need not be equal to $I_t$ because of the interference between the deformation potential and the electro-optic contributions to the scattering. The electro-optic effect depends on the strength of the ionic field which vanishes for the TO branch for wave vector much greater than $\epsilon_0^{1/2}\omega_0$. Analysis of the data in Fig. 3 yields the following results for 5°K:

$$(I_l/I_t)=0.8\pm0.3,\quad \delta\omega_{\mathrm{FWHM}}=0.05\pm0.01\ \mathrm{cm}^{-1},$$
$$\tilde{\omega}_0=0.02\pm0.01\ \mathrm{cm}^{-1},$$

where $\delta\omega_{\mathrm{FWHM}}$ is the full width at half maximum of the Raman linewidth. The doublet is unresolved, and the splitting can only be determined by the broadening of the [110] spectrum.

From these values and the dielectric constant Eq. (12), we plot the dispersion relations for the 128-cm$^{-1}$ polariton in Fig. 4. The solid line represents the real part of $\epsilon(\omega)$ in the presence of the measured damping. The dashed curve is the lossless dispersion which predicts the peak frequency of the Raman line for a given scattering wave vector transfer $q$.

The room-temperature oscillator strength as measured by Russell and Bell[24] using far-infrared spectroscopy yields a splitting $\tilde{\omega}_0=0.1$ cm$^{-1}$. Plendl *et al.*[25] show that this strength decreases on lowering the temperature.

Before plotting the temperature dependence of the shifts and linewidths, it is useful to have a picture of

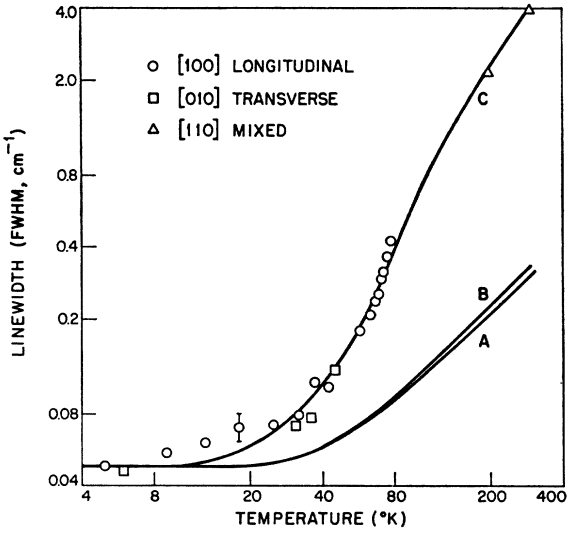


FIG. 7. Raman linewidth of 128-cm$^{-1}$ mode in $\alpha$-quartz. The solid curve $A$ is $\Gamma_{132}=(2n_{66}+1)0.048$. The solid curve $B$ is $\Gamma_{132}=(2n_{66}+1)0.048F(\eta,\delta)$. The solid curve $C$ is $\Gamma_{132}=(2n_{66}+1)0.048+(n_{60}-n_{132})0.1+(n_{132}-n_{266})1.0+(n_{266}-n_{398})12.0$.

[23] R. Loudon, Advan. Phys. 13, 423 (1964).

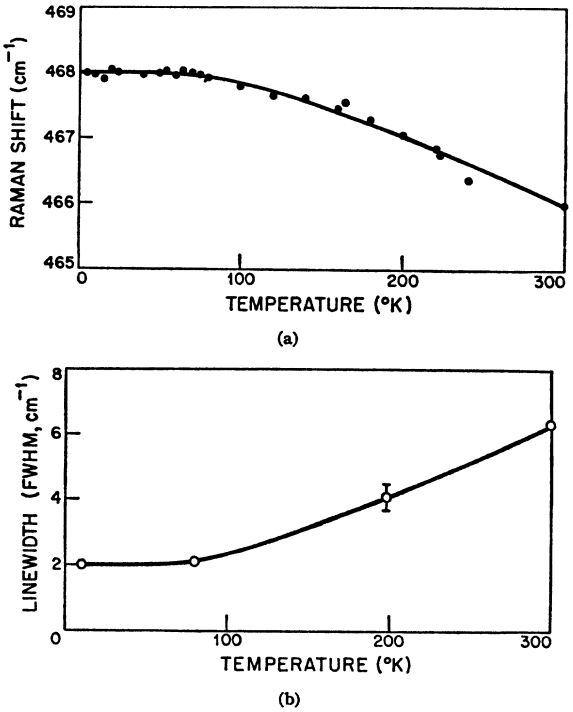


FIG. 8. (a) Raman shift of 466-cm$^{-1}$ mode in $\alpha$-quartz. The solid curve is $\Delta_{468}=(2n_{207}+1)1.72$. (b) Raman linewidth of 466-cm$^{-1}$ mode in $\alpha$-quartz. The solid curve is $\Gamma_{468}=(2n_{234}+1)2.0+(n_{207}-n_{673})4.4$.

[24] E. E. Russell and E. E. Bell, J. Opt. Soc. Am. 57, 341 (1967).

[25] J. N. Plendl, L. C. Mansur, A. Hadni, F. Brehat, P. Henry, G. Morlot, F. Noudin, and P. Strimer, J. Phys. Chem. Solids 28, 1589 (1967).

the phonon dispersion in order to establish possible damping routes. We present in Fig. 5 a schematic diagram of selected phonon branches in quartz; it is a composite of the neutron-scattering data and model calculations of Elcombe[2] and other Raman and infrared data. Representative decay channels and scattering processes are indicated. Other routes are available but they are either redundant (such as decay of the 128-$cm^{-1}$ mode to other acoustic branches) or unimportant for the temperature range of this experiment. Anisotropy and anharmonic selection rules are not considered although there is an apparent tendency for modes of like symmetry to interact most strongly. The symmetry imposed on the wave vectors of the interacting phonons by the $\mathbf{q}=0$ observed phonon relegates possible Umklapp processes to only those routes involving zone-edge phonons. For such rare processes there is a simple twofold degeneracy as a reflection of one zone-edge phonon about $\mathbf{q}=0$ results in an allowed normal process.

The shifts and linewidths for the 128-$cm^{-1}$ and 466-$cm^{-1}$ modes are shown in Figs. 6, 7, and 8. The temperature dependences are fit to the factors noted in the captions in units of $cm^{-1}$ making use of the theory of Sec. 2 A. Generally it should be noted that more terms are required to fit the lineshape data than the shifts. This reflects the lack of freedom in choosing the residual low-temperature width since it is directly measurable. The unobservable residual shift, however, may be treated as an adjustable parameter. Also, the energy conservation restriction limits the influence of any particular damping channel, whereas the shift may be dominated by a few modes near resonance.

From the data on the 128-$cm^{-1}$ linewidth we may test our model Eq. (8). If we assume that the decay proceeds only to the longitudinal acoustic branch, then the measured residual width is given by $\Gamma_0^0$, where $\gamma\sim 20$ for the quartz lattice constant $c_0\simeq 5$ Å. This is a reasonable value for the Grüneisen constant considering that its magnitude is shared by the decay channels to the other acoustic branches.

Curve $A$ of Fig. 7 is the total contribution of the decay processes to the damping if the acoustic modes are undamped. However, the high-energy acoustic phonons are known to have a finite lifetime which may be estimated from thermal conductivity and ultrasonic absorption measurements.[19] Curve $B$ of Fig. 7 results for the realistic estimate $\eta=T/20\ 000$. It is seen that the acoustic broadening has little effect on the over-all damping. Finally, curve $C$ takes into account scattering processes by thermally excited phonons in addition to the decay channels, and the dressing of the thermal phonons has been neglected. As might be expected, these scattering processes make a crucial contribution to the linewidth at higher temperatures, and, in fact, the calculated curve is in fairly good agreement with the experimental data. Similar fits were obtained for the 466-$cm^{-1}$ vibration as seen in Fig. 8.

The complexity of processes which contribute to the anharmonic interaction in quartz is thus deciphered rather satisfactorily. The analysis of the calcite data by Park[10] suffered from the lack of phonon-dispersion data and the neglect of scattering processes. This apparently forced him to fit the data with a lopsided breakup of the 1086-$cm^{-1}$ vibration into a 1085-$cm^{-1}$ and a 1-$cm^{-1}$ mode. Ralston *et al.*[11] did not attempt to analyze their data on silicon and gallium arsenide although a rather specific theory had been proposed by Klemens[17] for silicon.

## ACKNOWLEDGMENTS

We are grateful to F. H. Perry for expert technical assistance with the stimulated-Raman-scattering measurements. We also greatly appreciate the help of N. D. Strahm with the spectrometer experiment and for some clarifying discussions on polariton Raman intensities.